Automation, Control and Intelligent Systems
2013; 1(2) : 24-33
Published online April 2, 2013 (http://www.sciencepublishinggroup.com/j/acis)
doi: 10.11648/j.acis.20130102.12

Computer-aided diagnosis of pneumoconiosis X-ray images scanned with a common CCD scanner

Koji Abe[1,*], Takeshi Tahori[2], Masahide Minami[3], Munehiro Nakamura[4], Haiyan Tian[5]

[1]Kinki University, Osaka, Japan
[2]Contec EMS, Co. Ltd, Japan
[3]the University of Tokyo, Japan
[4]Kanazawa University, Kanazawa, Japan
[5]Chongqing University, Chongqing, China

Email address:

koji@info.kindai.ac.jp (K. Abe), tks_thr@outlook.com (T. Tahori), maminami@dream.com (M. Minami) , nakamura.kanazawa.u@gmail.com (M. Nakamura), haiyantian@cqu.edu.cn (H. Tian)

To cite this article:

Koji Abe, Takeshi Tahori, Masahide Minami, Munehiro Nakamura, Haiyan Tian. Computer-Aided Diagnosis of Pneumoconiosis X-ray Images Scanned with a Common CCD Scanner. *Automation, Control and Intelligent Systems*. Vol. 1, No. 2, 2013, pp. 24-33.
doi: 10.11648/j.acis.20130102.12

Abstract: This paper presents a discrimination of pneumoconiosis X-ray images obtained with a common CCD scanner. Current computer-aided diagnosis systems of pneumoconiosis have been proposed to images obtained with a special scanner such as a drum scanner or a film scanner for X-ray pictures. However, since the special scanners need a large storage space and the scanners and commitment of the imaging need high-priced costs, the systems are not practical in small clinics. In this paper, we propose features for measuring abnormalities of pneumoconiosis as variables for the discrimination. Devices in the proposed system are only a tablet PC and a CCD scanner. In images obtained with CCD scanner, abnormal levels of pneumoconiosis could depend on density distribution in rib areas. Therefore, the proposed method measures the abnormalities by extracting characteristics of the distribution in the areas. Besides, using the abnormalities, the proposed method discriminates chest X-ray images into normal or abnormal cases of pneumoconiosis. Experimental results of the discriminations for 59 right-lung images have shown that the proposed abnormalities are well extracted for the discrimination.

Keywords: Computer-Aided Diagnosis; Pneumoconiosis; Chest X-Ray Images; Medical Image Processing

1. Introduction

Pneumoconiosis is an interstitial lung disease caused by inhaling fine particles. In diagnosis of pneumoconiosis, diagnosticians judge pneumoconiosis reading small round opacities appeared on chest X-ray pictures. Pneumoconiosis is categorized into categories 0-4 according to profusion of small round opacities. Normal cases belong to category 0, where the opacities are not observed visually. And, abnormal cases belong to category 1, 2, 3, or 4, where the most serious level is category 4 and the opacities are observed most in category 4. Diagnosticians judge pneumoconiosis according to the criteria and the standard pneumoconiosis pictures prepared to every category. The criteria and the standard pictures are defined in the ILO (International Labour Organization). Like Japan, some countries have separately prepared the standard pictures and the criteria according to the criteria in ILO. However, since it is difficult for even experts on pneumoconiosis to diagnose pneumoconiosis, disagreement between diagnosticians is often happened. For the reasons, some CAD (Computer-Aided Diagnosis) systems for pneumoconiosis have been proposed.

The current CAD systems for pneumoconiosis are broadly distinguished into two ways: the one measures the abnormalities extracting features obtained by texture analysis[1], another one extracts small round opacities from lung images and measures their size and number as well as the real diagnosis by doctors[2]-[4]. All the systems were proposed to images obtained with a special scanner such as a drum scanner or a film scanner. Therefore, in order to practically use the systems in general hospitals, it is necessary to put the special scanners, or to order scanning chest X-ray pictures to a printing company in spite of high costs.

On the other hand, CAD systems for discriminating pneumoconiosis into normal and abnormal cases[5, 6] have been proposed to chest X-ray images obtained with a CCD scanner. In their evaluation experiments, abnormal lung images were obtained only from the standard pneumoconiosis pictures provided by Ministry of Health, Labour and Welfare in Japan. Since the number of the standard pneumoconiosis pictures is small for evaluations, the effectiveness of the CAD systems to actual abnormal cases is not confirmed. Moreover, the existing CAD systems[1]-[4] can not be applied to chest images obtained with CCD scanners because contrast of the shadow in the images is much unclear than the special scanners and the small round opacities are not appeared clearly. In order to practically use the CAD systems[5, 6] in general hospitals, this paper presents a discrimination of actual pneumoconiosis X-ray images obtained with a common CCD scanner. In addition, since results of the discriminations in the CAD systems[5, 6] are depended on noises such as shadows of blood vessels, ribs, and etc., this paper presents a method of reducing the affect of such noises.

2. Categorization of Pneumoconiosis X-Ray Images

The criteria for diagnosis of pneumoconiosis are defined in the Japanese Pneumoconiosis Law in accordance with criteria of pneumoconiosis in ILO. In the criteria, the severity of pneumoconiosis is indicated by profusion of small round opacities, where categories 0--4 have been established. Normal pictures belong to category 0, where the opacities are not observed visually. And, abnormal ones belong to category 1, 2, 3, or 4, where the most serious level is category 4 and the opacities are observed most in category 4. Patients diagnosed as pneumoconiosis are to be covered by the worker's compensation. In the diagnosis of pneumoconiosis, diagnosticians compare chest X-ray pictures with the standard pictures provided by ILO or Ministry of Health, Labour and Welfare in Japan. The latter one is predominately used in Japan.

Figure 1 shows the standard pictures and sketches provided by the ministry. In the sketches of category 1, 2, and 3, black specks indicate small round opacities and they increase as the category levels become higher. However, as shown in the standard pictures in Figure 1, the small round opacities do not appear clearly. In addition, since density is conspicuously high like noises at intersections of edges of other objects such as blood vessels, ribs, etc., it is very difficult for even medical doctors to read small round opacities. Although medical doctors diagnose pneumoconiosis according to the criteria and the standard pneumoconiosis pictures prepared to every category, their own experience much depends on the diagnosis because they need to observe subtle difference between a target and the standard pictures visually in the diagnosis.

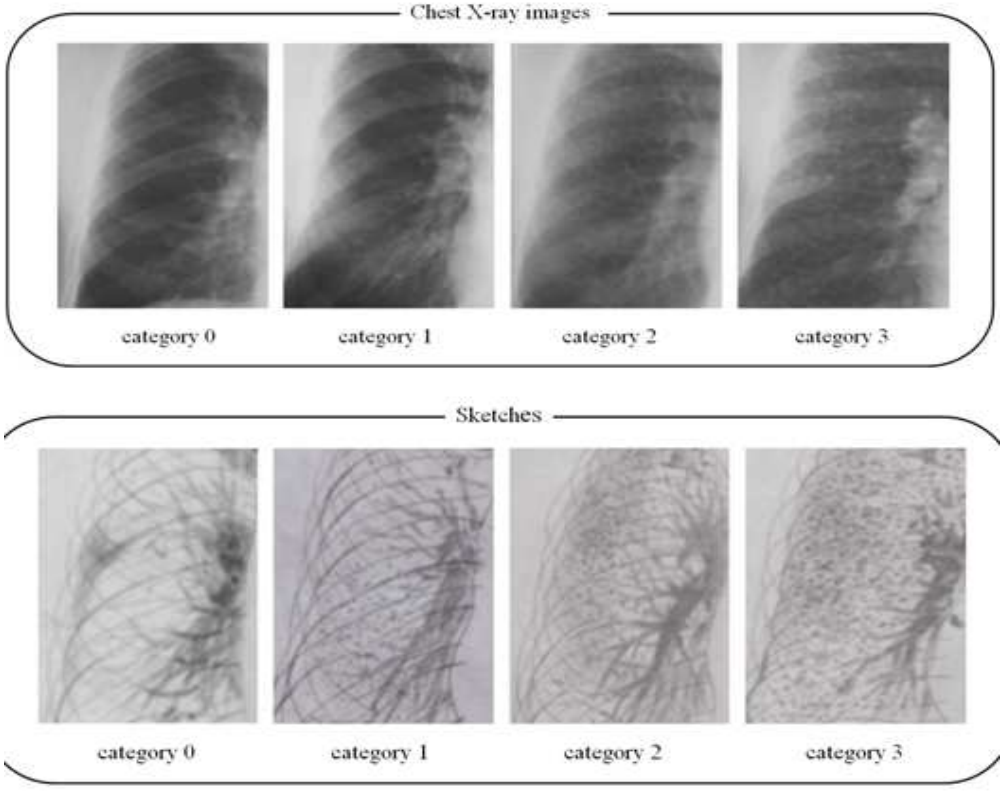

Figure 1. *The standard pneumoconiosis X-ray images scanned with a drum scanner (the first line) and the handwritten sketches for each of the images drawn by a diagnostician in pneumoconiosis (the bottom line). All of them are opened from Ministry of Health, Labour, and Welfare in Japan to the public.*

3. Density Distribution between Pneumoconiosis Pictures Obtained with CCD Scanner and Drum Scanner

Figure 2 shows a chest X-ray image obtained with a drum scanner and a histogram of pixel values in the part shown in the image. On the other hands, Figure 3 shows a chest image obtained with a CCD scanner and a histogram of pixel values in the part shown in the image, where the chest picture (category 2) for the image is the same one shown in Figure 2 and the location of the part is also the same as Figure 2. The chest images in Figure 2 and Figure 3 are configured with 300 dpi and 256 gray levels. Unlike the image obtained with drum scanner, we can see shadow of the ribs and small round opacities are unclear in the image obtained with CCD scanner, and the whore density values are much lower in the lung area. Table 1 shows statistics of the two histograms. From the table, we can see characteristics of the image obtained with a CCD scanner are quite different from the image obtained with a drum scanner even though their source is the same picture.

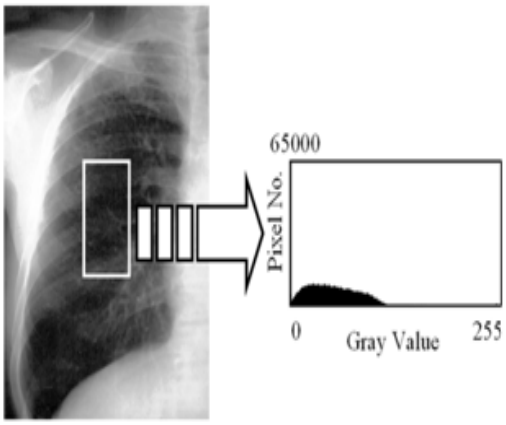

***Figure 2**. The chest image obtained with a drum scanner and the histogram obtained from the region of the white flame.*

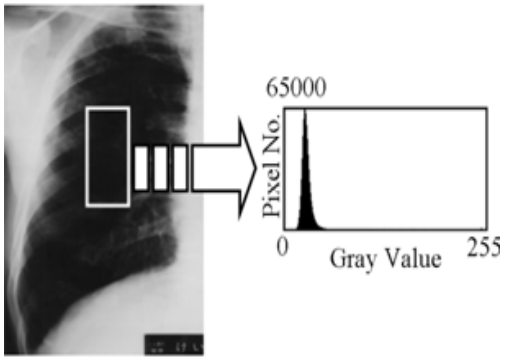

***Figure 3**. The chest image obtained with a CCD scanner and the histogram obtained from the region of the white flame.*

***Table 1.** Statistics of the histograms in Figure 2 and Figure 3.*

	Figure 2 (Drum scanner)	Figure 3 (CCD scanner)
Mean	87.4	26.5
St. Dev.	13.2	5.7
Skewness	0.8	1.9
Kurtosis	0.2	13

Thus, since CCD scanner can not accurately reproduce permeable films such as pictures, the visibility of lung in the image obtained with CCD scanner is considerably lower than drum scanner. For the reason, it is suggested that the existing system[1] can not extract small round opacities from chest X-ray images obtained with CCD scanner. Similarly, since the texture analysis is significantly affected by the image quality, texture analysis[2]-[4] could not effectively extract features from the images. Therefore, it would be necessary to propose a novel method to design a CAD for pneumoconiosis in picture images obtained with CCD scanner.

4. Proposed Method

4.1. Overview

Comparing with category 0, small high density regions assumed as small round opacities appear a lot in rib areas in images (obtained from a CCD scanner) of category 1, 2, and 3. Therefore, in the proposed method, abnormalities of pneumoconiosis are measured by extracting characteristics of the density distribution in rib areas. A method for extracting rib areas in chest X-ray images has been reported[7]. However, as shown in Figure 3, this method could not be applied for the unclear images scanned with a CCD scanner as well as the existing CAD systems of pneumoconiosis. Hence, in the proposed method, the rib areas are manually designated using a tablet PC. Since diagnosticians in pneumoconiosis judge few cases in one time, a dialogical system such as for one case in pneumoconiosis diagnosis is practical for general usage.

First, in the proposed method, the right lung area in chest X-ray pictures is digitalized by a CCD scanner. Next, the chest image is displayed on the tablet PC and the user draws curves along the edges for shadows of ribs on the image using the tablet PC. And then, the rib areas are designated using the drawn curves. Finally, abnormalities of pneumoconiosis are extracted from the rib areas. The extracted abnormalities are used as valuables for discrimination of chest X-ray images into normal or abnormal cases in pneumoconiosis.

4.2. Preprocessing

First, the right lung area in chest X-ray pictures (35 cm×35 cm) is digitalized by a CCD scanner, where all the

functions on the image filtering are turned off. The digitalized chest image is configured with 300 dpi and 256 gray levels. Next, the image is resized into 1000 pixels in height without changing the aspect ratio. And then, in order to standardize the range of the density value in each image, the histogram stretching is applied to each image as below where v' is the density value after the transition and v is the density value before the transition. And, regarding $hist[i]$ as the number of density value i (i=0,1,…,255) and $hist[max]$ as the maximum value in $hist[0] \sim hist[255]$, a is a natural value from 0 to max, where $hist[a]$ has the nearest value of $hist[max]/3$ in $hist[0] \sim hist[255]$. And, b is a natural value from max to 255, where $hist[b] = 0$ and $hist[max] \sim hist[b\text{-}1]$ is greater than 0. Figure 4 shows an example of parameter $hist[max]$, a, and b.

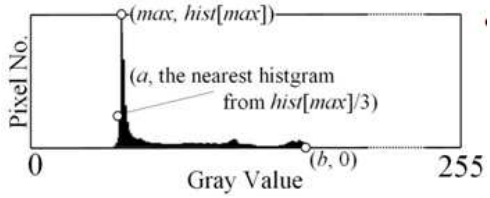

Figure 4. *The density histogram extracted from a chest X-ray image where the histogram stretching is not applied.*

4.3. The Density Histogram Extracted from a Chest X-Ray Images Where the Histogram Stretching is not Applied.

First, the chest image obtained in 4.2 is displayed on the tablet PC and the user draws 8 curves with white color along the edges for shadows of 4 ribs on the image using the tablet PC. Here, setting the thickness of the curves as 4 pixels, the drawn curves would cover the actual rib edges. Although there are 6 shadows of ribs in the image, the uppermost rib area and the bottom rib area are not designated because shadows of back bones and blade bones are often covered on the uppermost rib area and the bottom rib area is often unclear significantly. The manual for drawing the curves is described as below.

[The Manual for Drawing Curves for the Rib Edges]

(1) Open the right lung image prepared in 4.2 with paint tool.

(2) Select the round brush and configure the thickness of the circle as 4 pixels.

(3) Configure the line color as white.

(4) Start drawing the curve for an edge from the outside curve shown in Figure 5 along with shadows of the rib.

(5) Stop drawing the curve around a location where the edge can hardly be seen. Figure 5 (c) shows an example of drawn curves.

According to the manual above and the example of drawn curves in Figure 5, the user draws the curves. Figure 6 shows the procedure for designating the rib areas. First, pixel values of the drawn curves in Figure 6 are quantized as 255 (white) and the other parts are quantized between 0 and 254 in advance. Then, only the drawn curves are extracted by the labeling for pixel value of 255 as shown in Figure 6 (b). Figure 6 (c) shows the rib areas R_1-R_4 extracted from Figure 6 (b). Each of the areas is designated by the following. First, a pair of the upper and lower edge as shown in Figure 7 is regarded as neighbor edge in this paper. Then, the cutoff line in Figure 7 is drawn as it covers a neighbor edge. Next, shifting the cutoff line to the inside of the lung horizontally while the line and both of the upper and lower edge cross over, the boundary for the rib area is configured. Appling this procedure to all the pair of neighbor edges, Rm (m: 1 ～4) is designated. In Figure 7, the first line is regarded as k-th scanning line (k=1) and the value k is added by 1 whenever the scanning line is shifted to the right by 1 pixel. Besides, the uppermost pixel on k-th scanning line is regarded as j = 1 and the value j is added by 1 whenever the pixel goes down by 1 pixel.

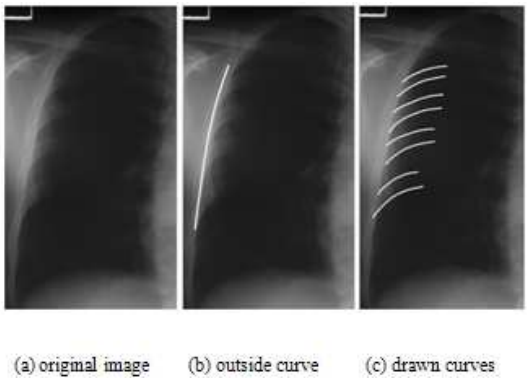

Figure 5. *Drawn curves for the rib edges.*

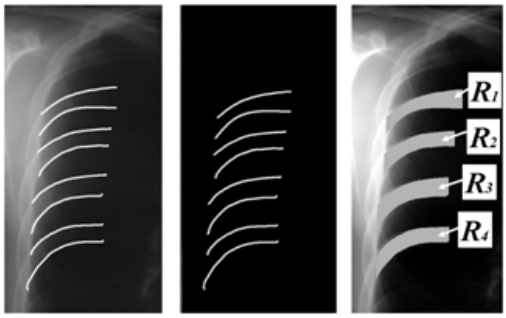

Figure 6. *Designated rib edges (R_1-R_4).*

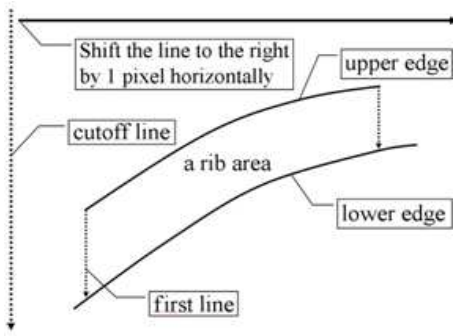

Figure 7. *Designation of a rib area.*

$$v' = \begin{cases} 0 & (0 \le v < a) \\ 255 \times \dfrac{v-a}{b-a} & (a \le v \le b) \\ 255 & (b < v \le 255) \end{cases} \quad (1)$$

4.4. Extraction of Abnormalities

Although small round opacities appear uniformly in chest X-ray pictures, they are unclear in images obtained with CCD scanner. However, it is obvious that the number of high-density small regions such as shadows of small round opacities and vessels increase according to the category level as shown in Figure 1. Hence, abnormalities of pneumoconiosis are extracted based on difference between pixel values in the regions and others. However, in the case when shadows of ribs overlap, abnormalities become high due to difference of the pixel value between two pixels even when high-density small regions are not covered on *k*-th scanning line. Figure 8 shows two pixel values on 8th scanning line in a rib area of category 1. As Figure 8 shows, although there are no small round opacities on the line, the difference of the pixel values between two pixels is up to 60. Figure 9 (a) shows density values of *j*-th scanning spot *v*[*j*] on the scanning line. And, Figure 9 (b) shows the dif ference of pixel values between *v*[*j*] and *v*[*j*+1] in Figure 9 (a). From Figure 9 (b), we can see the density value becomes lower as *j* increases until *j* = 24. However, from *j* ≧ 25, both of the positive and negative value are appeared 7 times alternatively and we can see the density distribution from *j* =25 is different from that of *j* = 1 ～ 24. Considering the characteristic, the proposed method divides the set of all the pixels on *k*-th scanning line into two, as its boundary is configured on the pixel where the density distribution changes. Then, the variance of pixel values in each of the sets is calculated. The boundary is configured on each of *k*-th scanning lines. And then, in order to enhance the difference of density distributions in two sets, the histogram stretching is applied to *k*-th scanning line in *Rm*. Figure 9 (c) shows density values on the scanning line where the histogram stretching is applied. Then, regarding *tm*[*k*]-th pixel counted from the uppermost edge as the boundary, the discriminant analysis is conducted to divide the set of *j* = 1 ～ *tm*[*k*]-1 and *j* = *tm*[*k*] + 1 ～ *heiRm*[*k*].

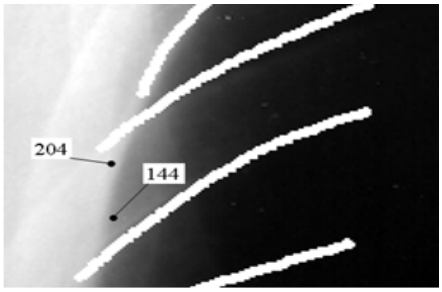

Figure 8. *Pixels values at some locations in a chest X-ray image (category 0) obtained with a CCD scanner.*

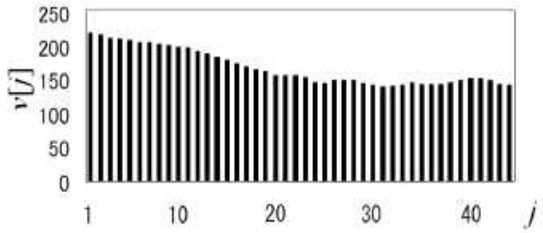

(a) Density values on the 8-th scanning line in a rib area.

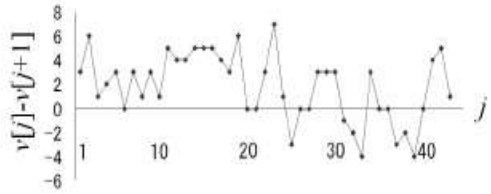

(b) Difference of density values between the neighbor pixels in (a).

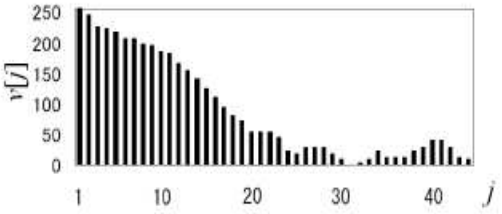

(c) Density values after the histogram stretching applied to (a).

Figure 9. *Pixels values at some locations in a chest X-ray image (category 0) obtained with a CCD scanner.*

Figure 10 shows parameters for extracting the abnormality of *k*-th scanning line in *Rm*, where *heiRm*[*k*] is the width of the *k*-th scanning line. As the scanning is conducted from the upper edge to the lower edge along with the scanning line, the abnormality of *k*-th scanning line in *Rm* is defined as

$$Abn(Rm[k]) = \left[\frac{1}{heiRm[k]-1} \left(\sum_{j=1}^{heiRm[k]} |v[j] - avg[k,j]|^2 \right) \right]^{\frac{1}{2}} \quad (2)$$

Where

$$avg[k,j] = \begin{cases} \text{if} \quad 1 \le j < tm[k], \\ \quad \left(\sum_{i=1}^{tm[k]-1} v[i] \right) / (tm[k]-1) \\ \text{if} \quad j = tm[k], \\ \quad v[j] \\ \text{if} \quad tm[k] < j \le heiRm[k], \\ \quad \left(\sum_{i=tm[k]+1}^{heiRm[k]} v[i] \right) / (heiRm[k] - tm[k]) \end{cases} \quad (3)$$

Next, as the first scanning line in *Rm* shifts pixel by pixel to the most inside of the scanning line horizontally, the abnormality in *Rm* is defined as

$$Abn(Rm) = \frac{1}{widRm}\left(\sum_{k=1}^{widRm} Abn(Rm[k])\right) \quad (4)$$

where *widRm* is the number of the horizontal shifts. Then, the abnormality in the whole rib areas is defined as

$$AbnR = \frac{1}{L_R}\left(\sum_{m=1}^{4}\sum_{k=1}^{widRm} Abn(Rm[k])\right) \quad (5)$$

where

$$L_R = \sum_{m=1}^{4} widRm \quad (6)$$

In addition, the maximum value among $Abn(R_1)$ - $Abn(R_4)$ is represented as *AbnRMAX*. Thus, *AbnR* represents overall abnormalities of pneumoconiosis in rib areas and *AbnRMAX* represents local abnormalities of pneumoconiosis in all the rib areas. The proposed abnormalities are based on doctor's experience that they consider comprehensive appearance of small round opacities in lung as well as appearance of each opacity. Figure 11 shows pixel values at some locations in a chest picture of category 0. From the figure, we can see the density value becomes lower towards the inside of the lung. Hence, if we extract abnormalities of pneumoconiosis not using the vertical scanning line, $Abn(Rm[k])$ would rather depend on density distribution in lung.

Seeing the concept of the proposed method, the proposed method could be regarded as a texture analysis method focusing on difference of contrast between small areas. It means the proposed method could be applied in problems to conduct texture analysis. Especially, differing from general texture analysis methods such as fractal dimension, run length matrix, etc., the proposed method decreases dependence of the horizontal gradation in an area to the abnormalities since the proposed method measures the variance of pixel values in each vertical scanning line. In addition, the proposed method can be applied even if the gradation in an area is occurred in the vertical direction and the scanning lines are in horizontal direction.

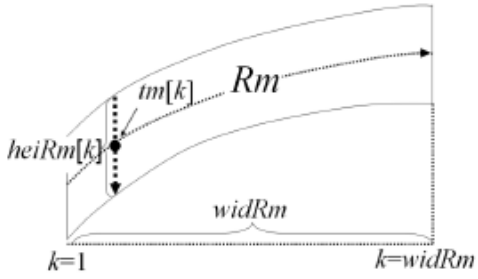

Figure 10. *Parameters for the extraction of Abn(Rm).*

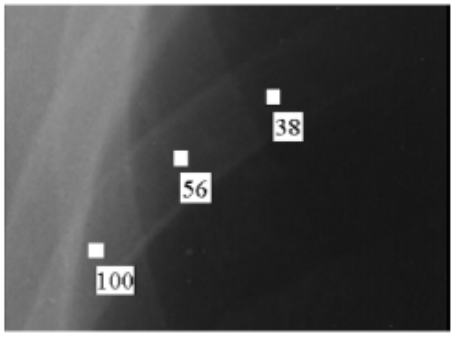

Figure 11. *Pixel values at some locations in a chest picture of category 0 obtained with a CCD scanner.*

5. Experimental Results

5.1. Results of the Abnormalities

The proposed abnormalities were extracted from 59 chest X-ray pictures. The X-ray pictures were scanned with a CCD scanner (Canon:CanoScan 8800F) and only the right lung in every of the pictures was obtained (resolution: 300 dpi, gray level: 8 bits, format: bitmap image). The number of X-ray images which belong in category 0 is 47, the number in category 1 is 5, the number in category 2 is 4 and the number in category 3 is 3. To obtain rib areas, each of an expert diagnostician and three non-experts (represented as userA, userB, and userC) in pneumoconiosis diagnosis drew the rib edges on all the chest images with a tablet PC (ThinkPad 200Tablet 4184-F5J). The total time used for drawing all the images was 48 minutes in the case of userA, 56 minutes in the case of userB, and 40 minutes in the case of userC. The total time for the expert could not be measured because he/she drew them in spare moments from his regular work. Figure 12 shows the abnormalities *AbnR* and *AbnRMAX* extracted from all the images. From the figure, we can see both of *AbnR* and *AbnRMAX* have been increased gradually according to increase of the category level.

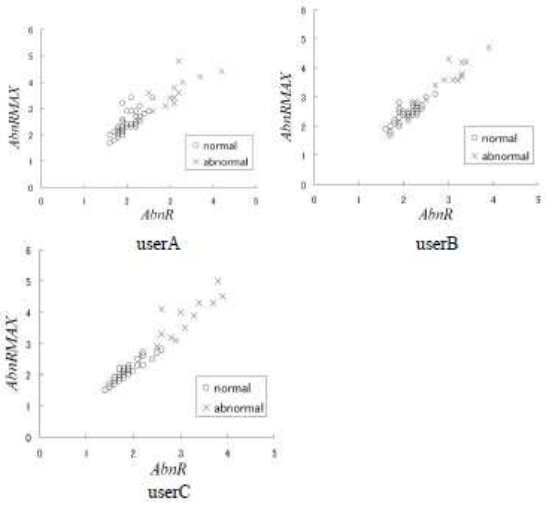

Figure 12. *AbnR and AbnRMAX of the 56 images.*

5.2. Discrimination of Chest X-Ray Images into Normal or Abnormal Cases

Since patients diagnosed as pneumoconiosis are to be covered by the worker's compensation, the discrimination into normal and abnormal cases in pneumoconiosis diagnosis is especially important for medical doctors. In the checkup of pneumoconiosis, if the diagnostician judges a patients picture as abnormal case, the picture comes on a committee of experts in pneumoconiosis. Then, when it is difficult to discriminate a target picture, disagreement between the diagnostician and the committee is often happened. For the reason, since it is difficult for even experts on pneumoconiosis to diagnose pneumoconiosis, CAD systems for pneumoconiosis have been required. Therefore, we examine performances of the proposed method by the discrimination of the X-ray images into normal or abnormal (i.e., pneumoconiosis) cases by regarding the abnormalities as variants, respectively. As the way of the discrimination, Linear Discriminant Random Trees (RT), a Neural Network (NN), a Support Vector Machine (SVM) were applied to the proposed abnormalities. The number of the trees in RT was set as 10. And, NN was designed as a three-layered perceptron (input layer: 2, hidden layer: 3, output layer: 1), where sigmoid function and the random search method by Matyas were used. Comparing with normal case, since the number of abnormal cases is small, training set and test set were chosen by the cross validation[8] in all the discriminations. The method of cross validation is often applied to increase the number of trials when the number of samples is small for evaluations. In fact, every discrimination was conducted as the following procedure:

(1) Choose N images from all the images as test data, and use the other images as training set.

(2) Discriminate the test data between category 0 and the other categories.

(3) Repeat the procedure from (1) to (2) to every combination changing the test data.

First, Table 2 shows the average recall (*Recall*) in the discriminations when N = 1. And, Table 3 shows the average precision (*Precision*) in the discriminations when N = 1. The brace notation in Table 3 shows the number of images used for calculation of *Recall* and *Precision*. *Recall* and *Precision* are defined as where, regarding H as the target category, $N_{category}$ is the number of images in H, $N_{correct}$ is the number of images discriminated correctly in H to all the test data (59 images), and N_{output} is the number of images discriminated as H to all the test data.

Next, in order to increase the number of trials for the discrimination, we examined performance of the proposed method when N = 3. Hence, ${}_{59}C_3$ = 32509 evaluation functions were prepared in the discrimination. Here, each image is included in test data for ${}_{58}C_2$ = 1653 times and the total number of trials is 59×1653 = 97257. The average recall (R_{avg}) and precision (P_{avg}) in the discrimination are shown in Table 4 and Table 5, respectively. R_{avg} and P_{avg} are defined

$$R_{avg} = \frac{|A_{output} \cap A_{category}|}{|A_{category}|} \times 100 \quad (9)$$

$$P_{avg} = \frac{|A_{output} \cap A_{category}|}{|A_{output}|} \times 100 \quad (10)$$

where A_{output} is the set of numbers in all the trials discriminated as H, where each of all the trials (97257) is numbered to avoid overlap. Hence, $|A_{category}|$ is the total number of images correctly discriminated in all the trials.

Table 2. *Recall and Precision for the existing method (N=1).*

		Normal		Abnormal	
User	Method	Recall	Precision	Recall	Precision
A	RT	93.62%	81.48%	16.67%	40.00%
	NN	97.87%	80.70%	83.33%	50.00%
	SVM	78.72%	80.43%	25.00%	23.07%
B	RT	87.23%	85.41%	41.67%	45.45%
	NN	70.21%	80.46%	33.33%	22.22%
	SVM	93.62%	88.00%	50.00%	66.70%
C	RT	93.61%	86.27%	41.67%	62.50%
	NN	93.62%	88.00%	50.00%	66.70%
	SVM	91.49%	89.58%	58.33%	63.63%

Table 3. *Recall and Precision for the proposed method (N=1).*

		Normal		Abnormal	
User	Method	Recall	Precision	Recall	Precision
A	RT	95.74%	95.74%	83.33%	83.33%
	NN	95.74%	95.74%	83.33%	83.33%
	SVM	95.74% (45/47)	95.74% (45/47)	83.33% (10/12)	83.33% (10/12)
	RT	95.74% (45/47)	95.74% (45/47)	83.33% (10/12)	83.33% (10/12)
B	NN	97.87%	97.87%	91.67%	91.67%
	SVM	97.87% (46/47)	97.87% (46/47)	91.67% (11/12)	91.67% (11/12)
	RT	97.87% (46/47)	97.87% (46/47)	91.67% (11/12)	91.67% (11/12)
C	NN	100.0%	97.92%	91.67%	100.0%
	SVM	97.87% (46/47)	100.0% (46/46)	100.0% (12/12)	92.31% (12/13)

5.3. Discussion

First, Table 6 shows the mean and standard deviation (SD) of *AbnR* and *AbnRMAX* extracted from each of the normal and abnormal images drawn by each user. From Table 6, we can see both of two abnormalities in abnormal cases are higher than those of normal cases, and the proposed abnormalities are appropriately extracted for the discrimination of pneumoconiosis.

Next, we consider results of the discrimination shown in 5.2. First, the result of the discriminations in Table 3 and 5 is similar to each other. Besides, from experimental results

obtained by the existing method shown in Table 2 and 4, we can see both of *Recall* and *Precision* are increased by the proposed method as shown in Table 3 and 5. Although this is not rigorous comparison, since *Recall* of the discrimination in the existing systems[1]-[4] is Approximately from 60% to 80%, we can say the proposed method has high performance in the discrimination of pneumoconiosis. On the other hand, the accuracy of border line in diagnosis of pneumoconiosis is unclear because screening examina- tion is not conducted on pneumoconiosis. As an example, in screening examination of the Central Committee on Quality Control of Mammographic Screening, diagnosticians need to find breast cancer at 80% accuracy and judge the others as not cancer at 80% accuracy. Considering the case above, we can say the proposed method has high performance even from clinical point of view.

Table 4. *Recall and Precision for the existing method (N=3).*

		Normal		**Abnormal**	
User	Method	Recall	Precision	Recall	Precision
	RT	91.26%	81.45%	18.59%	35.19%
A	NN	98.30%	80.91%	9.2%	57.85%
	SVM	80.36%	62.20%	31.87%	29.29%
	RT	88.64%	84.02%	33.99%	43.32%
B	NN	99.03%	79.80%	1.8%	32.50%
	SVM	71.27%	82.24%	39.72%	26.09%
	RT	96.22%	87.36%	45.51%	75.43%
C	NN	94.50%	88.84%	83.50%	71.28%
	SVM	91.34%	89.57%	58.33%	63.22%

Table 5. *Recall and Precision for the proposed method (N=3).*

		Normal		**Abnormal**	
User	Method	Recall	Precision	Recall	Precision
	RT	95.81%	95.75%	83.35%	83.56%
A	NN	98.12%	95.55%	82.11%	91.79%
	SVM	95.97%	95.89%	83.90%	84.17%
	RT	96.36%	96.02%	84.37%	85.53%
B	NN	98.58%	97.33%	89.39%	94.14%
	SVM	97.87%	97.87%	91.67%	91.67%
	RT	97.57%	97.81%	91.44%	90.58%
C	NN	99.06%	97.99%	92.06%	96.17%
	SVM	97.80%	99.73%	98.97%	92.02%

Table 6. *Statistics of AbnR and AbnRMAX.*

Category	**User**	**AbnR**		**AbnRMAX**	
		Mean	**SD**	**Mean**	**SD**
	A	2.0	0.2	2.4	0.4
Normal	B	2.1	0.2	2.4	0.3
	C	1.8	0.3	2.0	0.3
	A	3.2	0.4	3.7	0.5
Abnormal	B	3.1	0.3	3.8	0.5
	C	3.1	0.5	3.8	0.6

We consider images discriminated incorrectly in experiments shown in 5.2. There are 2 images discriminated incorrectly as normal case when both of N = 1 and N = 3. Each of the images is represented as abnormal ① and abnormal② respectively in this paper. Figure 13～15 show the abnormalities *AbnR* and *AbnRMAX* extracted from all the images drawn by each user. abnormal① was discriminated incorrectly when N = 1 expect in the discrimination by SVM in the case of userC. Table 7 shows the total number of cases that abnormal ① was discriminated correctly in all the 1653 trials. From Figure 13～15, abnormal① has the lowest abnormality in all the images regardless of user. Figure 16 shows the standard deviation $SD[k]$ obtained from density values in all the pixels on k-th scanning line in R_4. And, Figure 17 shows $Abn(Rm[k])$ extracted from the density values in all the pixels on k-th scanning line in R_4. Although shadows of ribs overlap each other on scanning lines from k = 1 to 24, the average of $SD[1]$～$SD[24]$ is 10.2 in Figure 16 and the average of $Abn(Rm[1])$～$Abn(Rm[24])$ is 4.6. Since both of $SD[k]$ and $Abn(Rm[k])$ are based on average of density values in a set of pixels on a scanning line, we can see noises appeared from k = 1 to 24 in Figure 16 are reduced as shown in Figure 17. However, sometimes $Abn(Rm[k])$ does not become higher in the case when small round opacities on k-th scanning line appear only on the set of pixels, namely $j = 1 \sim tm[k]$-1 or $j = tm[k]+1 \sim heiRm[k]$ because the opacities are regarded as noise. For example, although the noise does not exist on 39 th scanning line in R_4, $SD[39]$ is 8.2 in Figure 16 and $Abn(Rm[39])$ is 5.0 in Figure 17. There is a gap of the average density value between the set of pixels $j = 1 \sim tm[39]$-1 and $j = tm[39] + 1 \sim heiRm[39]$ on the 39th scanning line, the former one is 87.7 and the latter one is 71.5.

Table 7. *Number of the cases that abnormal① was discriminated correctly.*

User	**Method**	**Correct results / Trials**	
	RT	4/1653	0.24%
A	NN	184/1653	11.13%
	SVM	3/1653	0.01%
	RT	0/1653	0%
B	NN	3/1653	0.01%
	SVM	0/1653	0%
	RT	12/1653	0.7%
C	NN	365/1653	22.08%
	SVM	1448/1653	87.60%

Table 8. *Number of the cases that abnormal② was discriminated correctly.*

User	**Method**	**Correct results / Trials**	
	RT	2/1653	0.12%
A	NN	147/1653	8.89%
	SVM	111/1653	6.71%
	RT	1653/1653	100%
B	NN	1621/1653	98.06%
	SVM	1653/1653	100%
	RT	1630/1653	98.61%
C	NN	1641/1653	99.27%
	SVM	1653/1653	100%

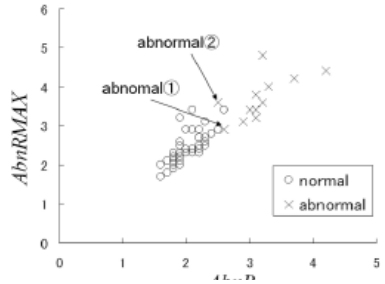

Figure 13. *abnormal① and abnormal② in the images drawn by userA.*

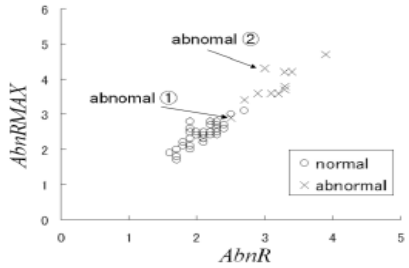

Figure 14. *abnormal① and abnormal② in the images drawn by userB.*

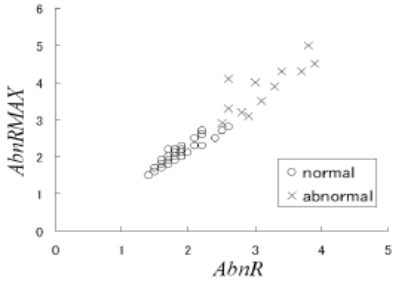

Figure 15. *abnormal① and abnormal② in the images drawn by userC.*

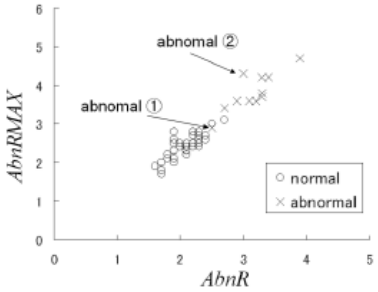

Figure 16. *SD[k] extracted from a rib in abnormal①.*

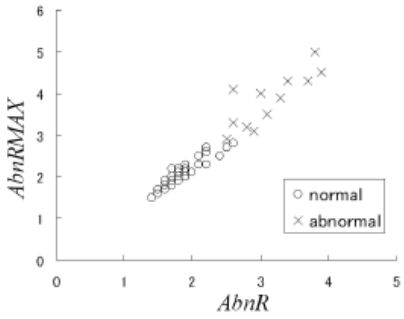

Figure 17. *Abn(Rm[k]) extracted from a rib in abnormal①.*

The gap indicates a small round opacity is appeared mostly on the set of pixels $j = 1 \sim tm[39]-1$, and variance of the density values in the set would be low. In this case, by detecting overlap of shadows of ribs on the scanning line, we would like to select $SD[k]$ or $Abn(Rm[k])$ as the abnormality on the scanning line. abnormal② was discriminated incorrectly by all the tools when $N = 1$. The total number of trials to abnormal② is 1653 when $N = 3$, and Table 8 shows the number of correctly discriminated cases by each tool in each user. From Figure 13～15, we can see the normal cases and abnormal cases can be broadly grouped, and abnormal② for userA in Figure 13 is placed around boundary between the two groups of normal case and abnormal case. From Table 8, since average correct ratio of abnormal② is significantly different between userA and the others, abnormal② for userA could be discriminated incorrectly according to the accuracy of the drawn curve. The above example is considered to be an example of the case that the proposed abnor-malities are depended on the accuracy of drawn curves. Hence, as a future subjective, to reduce the significant difference of drawn curves between users, we need to consider the way of displaying the manual and samples for drawing curves for the rib edges.

6. Conclusions

To enhance cost-performance and mobility in CAD systems for pneumoconiosis, this paper has presented a method for extracting abnormalities of pneumoconiosis from chest X-ray images obtained with a CCD scanner. The abnormalities have been extracted from rib areas based on density distribution in the areas. Then, regarding the abnormalities as variants in the discrimination of pneumoconiosis, this paper has examined performance of the proposed abnormalities with the common discriminations. Experimental results of the discriminations for 59 right-lung images have shown that both of the recall and precision has become more than 90% to the normal lungs and 80% to the abnormal lungs.

As future subjects, it is necessary to design an interface for drawing rib edges or propose a method for extracting rib areas automatically. And then, considering cases of discrimination failure, it is necessary to detect overlap of shadows of ribs on scanning lines, and to consider the manual and samples for drawing rib edges as the proposed method less depends on user.

References

[1] R. P. Kruger, W. B. Thompson, and A. F. Turner, “Computer diagnosis of pneumoconiosis,” Trans. on Systems, Man. And Cybernetics, vol. SMC-4, no. 1, pp. 40–49, Jan. 1974.

[2] A. M. Savol, C. C. Li, and R. J. Hoy, “Computer aided recognition of small rounded pneumoconiosis opacities in chest X-rays,” IEEE Trans Pattern Anal. March. Intell., vol. 2, no. 5, pp. 479-482, Sep. 1980.

[3] J. Wei and H. Kobatake, “Detection of rounded opacities on chest radiographs using convergence index filter,” Proc. ICIAP, pp. 757-761, Sep. 1999.

[4] H. Kondo and T. Kouda, “Computer-aided diagnosis for pneumoconiosis using neural network,” Proc. IEEE Symposium on Computer-Based Medical Systems, pp. 467-472, Jul. 2001

[5] M. Nakamura, K. Abe, and M. Minami, “Quantitative evaluation of pneumoconiosis in chest radiographs obtained with a CCD scanner,” Proc. of ICADIWT 2009, pp. 673-678, London, UK, Ang. 2009.

[6] M. Nakamura, K. Abe, and M. Minami, “Extraction of features for diagnosing pneumoconiosis from chest radiographs obtained with a CCD scanner,” Journal of Digital Information Management, vol. 8, no. 3, pp. 147-152, Jun. 2010.

[7] M. Loog and B. Ginneken, “Segmentation of the posterior ribs in chest radiographs using iterated contextual pixel classification,” IEEE Trans. on Medical Imaging, vol. 25, no. 5, pp. 602-611, May 2006.

[8] F. Mosteller, “A k-sample slippage test for an extreme population,” The Annals of Mathematical Statistics, vol. 19, no. 1, pp. 58-65, Mar. 1948.